EFFECT OF STRONG MAGNETIC FIELD ON PLASMA JET AT A LOW PRESSURE

Kazuo Koike*, Eiji Konno†, Norifumi Ono‡ and Ryoichiro Oshima*
Department of Mechanical Engineering,
Tohoku Gakuin University
13-1, Chuo-1, Tagajo, Miyagi, 985-8537, JAPAN

Abstract

An experimental study of a plasma jet at a low pressure was carried out to examine the controllability of the jet by the strong magnetic field. An argon gas was employed as a working fluid. The plasma jet was generated in a vacuum chamber by a high intensity DC arc discharge. The magnetic field was applied to the jet in the chamber by means of a pair of superconducting coils. The applied field was parallel to the jet axis. It was shown in the present observation that the jet width decreases with increases in the applied magnetic field and that the high temperature region is extended to downstream direction. Argon emission spectra were also measured to determine the excitation temperature of the jet. An optical probe was set at the middle between both coils. It was indicated from the relative line intensity measurement that the excitation temperature at the measuring position increases with the strength of magnetic field in the case that both coils operate. Thus, it was concluded that the high temperature region in the central part of the plasma jet becomes long as the field strength increases.

Introduction

It is promising that plasma propulsion will play an important role in the future space propulsion. It is also well-known that plasma is a typical example of functional fluids in the magnetic field[1]. Therefore, the performance of the propulsion system can be expected to improve remarkably, provided that strong magnetic field can be utilized for enhancing the functions of plasma flow. Experimental studies of functional enhancement of the plasma jet in the magnetic field have previously been made to examine the effects of magnetic field[2-4] and seeding[5] on the flow. However, data on the flow characteristics have not been obtained sufficiently under the strong magnetic field induced by a superconducting magnet. To realize the development of the plasma propulsion using strong magnetic field, it is important to get a better understanding of the plasma flow characteristics under wide ambient conditions.

From this point of view, in the present paper, the behavior of argon plasma jets in a vacuum chamber was shot through the windows for observation by a digital video camera when strong magnetic field was applied to the jet by means of a pair of superconducting coils. The relative line intensity measurement was also carried out to determine the excitation temperature of the jet.

Nomenclature

A_{ji} = Einstein coefficient for spontaneous emission
B = magnetic flux density
B_c = magnetic flux density between coils
E_j = energy of j level
g_j = degeneracy of j level
I_{ji} = spectral intensity of j to i transition
i_c = specified current of superconducting coil
i_s = supplied current to plasma torch
L = distance to optical probe from nozzle exit of plasma torch
$\dot{m}$ = mass flow rate
p = background pressure
T_{ex} = excitation temperature
λ_{ji} = wavelength of j to i transition

Subscripts
i = lower energy level
j = upper energy level

Experimental Setup and Procedure

The experimental setup used here is schematically shown in Fig.1. It is made up of 4 main systems; that is, a plasma generator system, a superconducting magnet system, an optical measuring system and a vacuum chamber with a vacuum pump system. Plasma jets were generated in the chamber by a high intensity DC arc discharge. The plasma torch can be moved along the centerline of magnet bore. The supplied current to the plasma torch i_s can vary between 70 and 300 A. An argon gas was employed as a working fluid. The behavior of the jets was shot

---

* Professor
† Graduate student
‡ Research Scientist

through three windows for observation installed on the side of the vacuum chamber by the use of a digital video camera. The chamber was evacuated to 2 Pa or less before measurements and held at a uniform pressure during measurements using the vacuum pump system. The background pressure in the vacuum chamber is maintained at about 410 Pa when the plasma jet is operating at a mass flow rate of 1.23g/s.

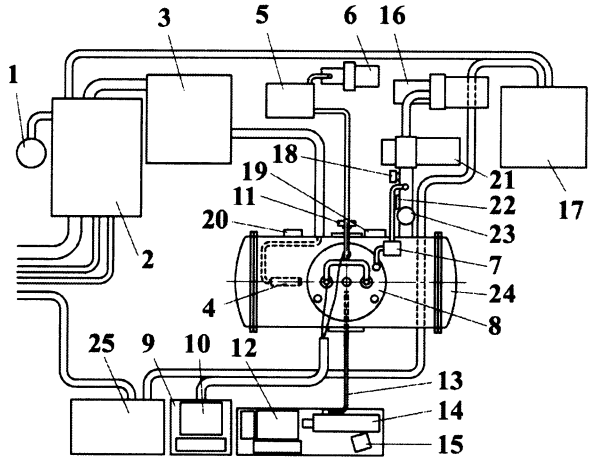

1. Argon gas cylinder
2. Power supply
3. Cooling system
4. Plasma torch
5. Oil diffusion pump
6. Rotary pump
7. Oil diffusion pump
8. Superconducting magnet system
9. Power supply
10. Computer system for magnet
11. Radiation thermometer
12. Computer system for optical system
13. Optical fiber cable
14. Optical multi-channel analyzer
15. Control unit
16. Rotary pump
17. Control panel (main)
18. Vacuum gauge
19. Pressure transducers
20. Gas inlet port
21. Mechanical booster pump
22. Spare port
23. Main valve
24. Vacuum chamber
25. Control panel

Fig. 1 Experimental setup

A magnetic field was applied to the jet by means of the superconducting magnet. The magnet consists of a pair of superconducting coils. Figure 2 indicates schematic view of cryostat. The cryostat holds the coils at liquid helium temperature. Upstream and downstream coils are named coil A and coil B, respectively. Each coil has the same specification and can produce a field in excess of 3 Tesla. Since it can operate individually, the field distribution can be changed. An example of the magnetic field distribution is shown in Fig. 3. The axial component of magnetic flux density was measured along the centerline of the magnet bore in the case that each coil operates at specified current i_c = 35.72A. The circle

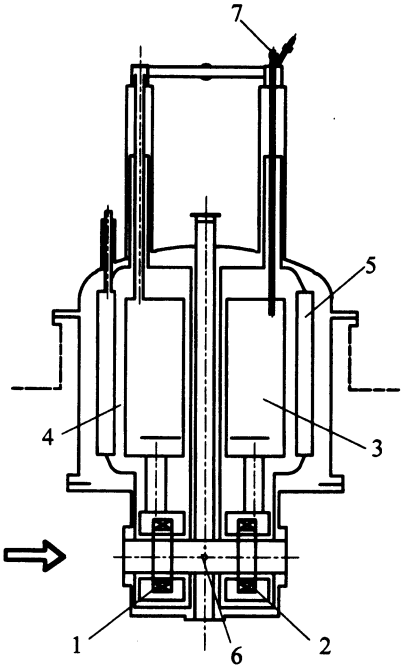

1. Coil A, 2. Coil B, 3. Liquid helium reservoir, 4. Vacuum insulation space, 5. Liquid nitrogen reservoir, 6. Measuring position, 7. Transfer tube entry port

Fig. 2 Schematic view of cryostat

mark denotes the magnetic flux density in the case that both coils operate. Data are represented by squares in the case that only upstream coil, coil A, operates. Data on downstream coil operation are illustrated by triangles. The magnetic flux density at the midpoint between coils, represented by z = 0 in this figure, is 0.5 T in the case that the both coils operate. The magnetic flux density at this point is referred to as B_c. It becomes 1.5 T under the condition of maximum specified current i_c = 107.16A.

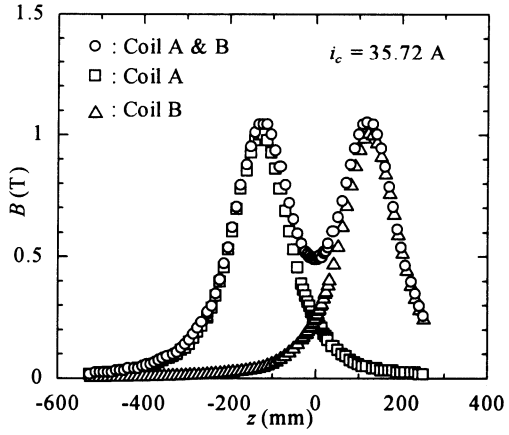

Fig. 3 An example of magnetic field distribution

Each measurement started after the pressure in the chamber became stable. The optical probe was set at the middle between coil A and B. Emission from the plasma jet was collected by the lens system at the head of the optical probe. The focused point was placed on the centerline of the plasma jet; that is, on the centerline axis of the magnet bore as illustrated in Fig. 4. The distance along the centerline between the torch exit and the focused point of optical probe, L, was fixed to a specified value before each measurement. The excitation temperature is determined on the basis of the relative line intensity measurement. That is, the emission collected from the plasma was transmitted to an optical multi-channel analyzer, Hamamatsu PMA-50, through an optical fiber cable. The monochromator in the optical multi-channel analyzer has three kinds of gratings. A 1200 gr/mm holographic grating, blazed 630nm, was mainly used for the present measurements. The data on the emission were calibrated using the relative spectral response of the optical system used here. On the basis of the corrected radiation intensity, the excitation temperature is determined using the following equation.

$$\frac{d\left[ln\left\{I_{ji}\lambda_{ji}/\left(g_j A_{ji}\right)\right\}\right]}{dE_j} = -\frac{1}{T_{ex}} \qquad (1)$$

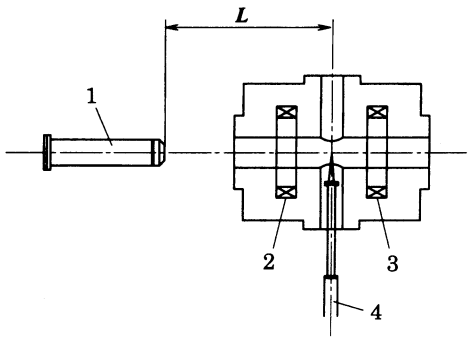

1. Plasma torch, 2. Coil A, 3. Coil B, 4. Optical probe

Fig. 4 Schematic view of measuring section

Results and Discussion

Figure 5 shows an example of plasma jet observed through the upstream window. These pictures in this figure were shot under the conditions of mass flow rate $\dot{m}$ =1.23±0.02 g/s, background pressure p =410±30 Pa, supplied current to the torch i_s =250 A and the distance from the torch exit to the focused point of optical probe L = 350mm. It is indicated from these pictures that the jet has a typical structure of under-expanded supersonic jet. That is, a Mach disk and a barrel shock are obviously formed. When the strong magnetic field is imposed to the jet, the width of bright part around closer region to the magnet reduces compared with that for no magnetic field. The width reduction becomes remarkable as the field strength increases. Moreover, the high temperature region, located in the middle of the jet and behind the Mach disk, becomes much bright.

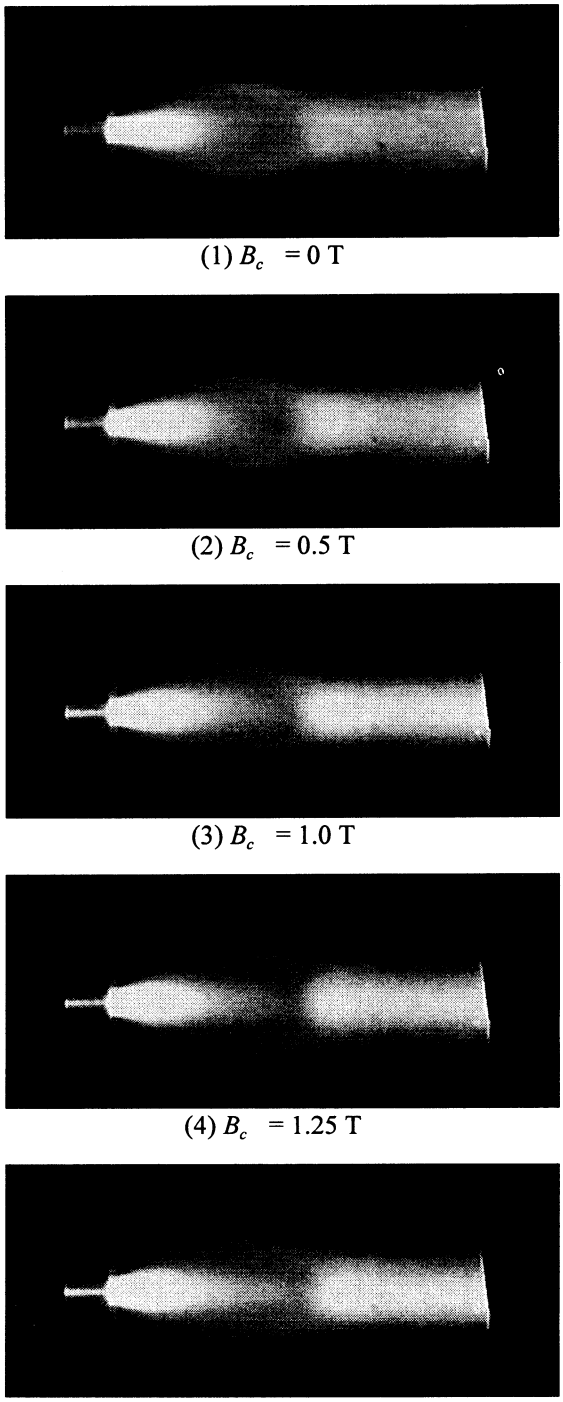

(1) B_c = 0 T

(2) B_c = 0.5 T

(3) B_c = 1.0 T

(4) B_c = 1.25 T

(5) B_c = 1.5 T

$\dot{m}$ =1.23±0.02 g/s, p =410±30 Pa, i_s =250 A and L = 350mm

Fig. 5 View through upstream window

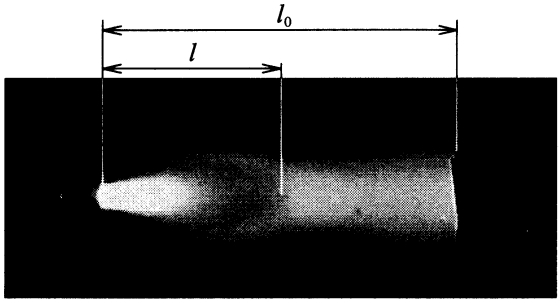

Fig. 6 Characteristic lengths l_0 and l

To examine the effects of the supplied current to the plasma torch and the intensity of magnetic field on the location of Mach disk, the distance to the Mach disk from the exit of the torch l was measured as illustrated in Fig. 6. Figure 7 shows the evolution of the Mach disk location with the supplied current to the plasma torch i_s. In this figure, the distance l is normalized to the distance between the torch exit and the end of the cryostat housing for the magnet l_0. The distance to the Mach disk from the exit of the plasma torch naturally increases with the supplied current to the torch.

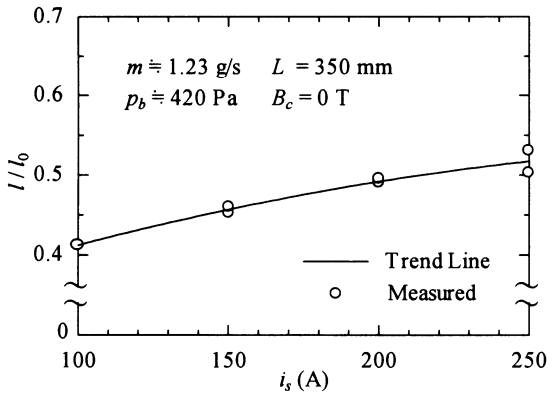

Fig. 7 Effect of the supplied current on the distance to Mach disk

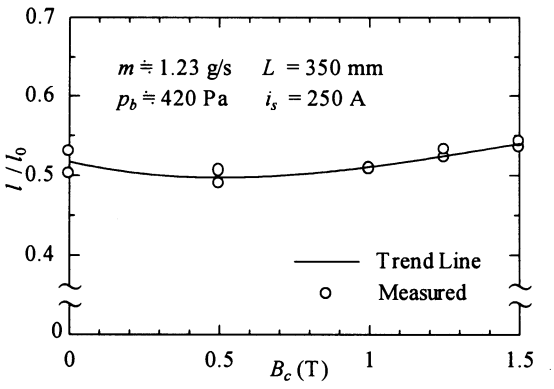

Fig. 8 Effect of magnetic field on the distance to Mach disk

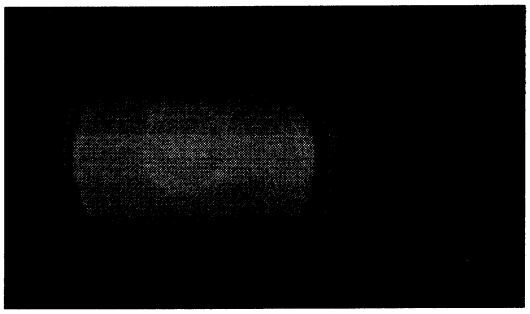

(1) B_c = 0 T

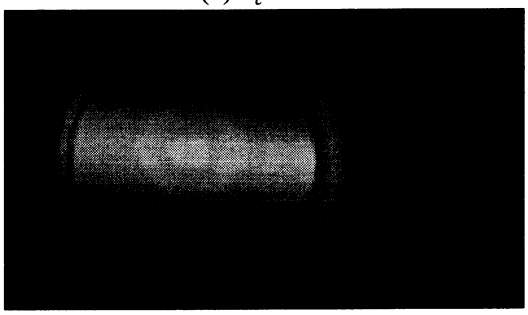

(2) B_c = 0.5 T

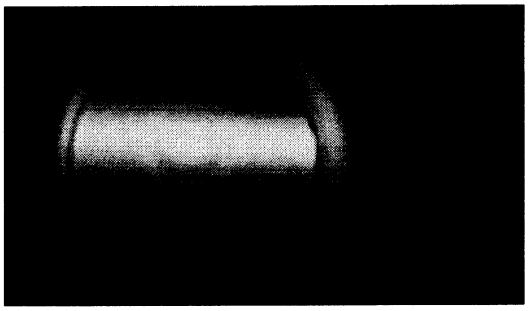

(3) B_c = 1.0 T

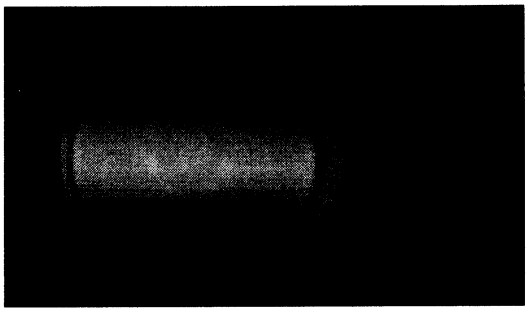

(4) B_c = 1.25 T

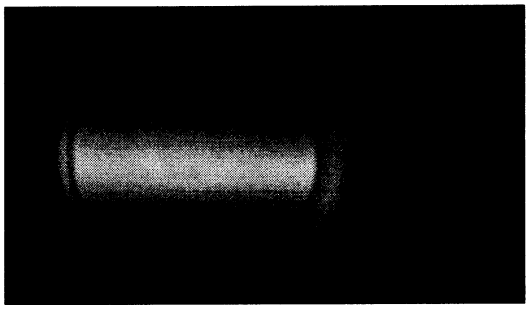

(5) B_c = 1.5 T

$\dot{m}$ =1.23±0.02 g/s, p =410±30 Pa, i_s =250 A and L = 300mm.

Fig. 9 View through center window

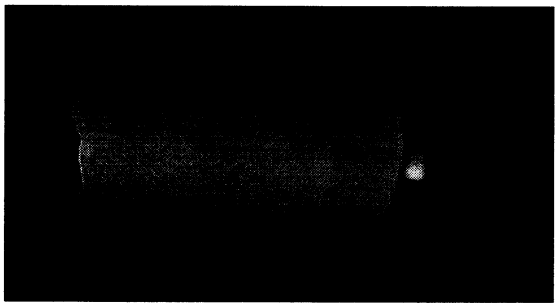

(1) B_c = 0 T

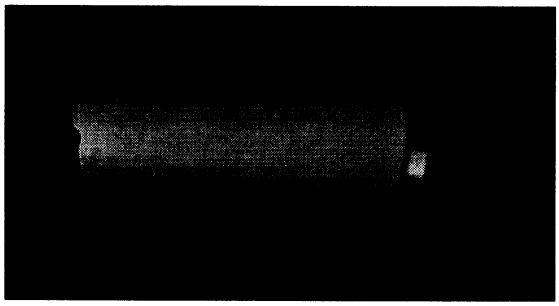

(2) B_c = 0.5 T

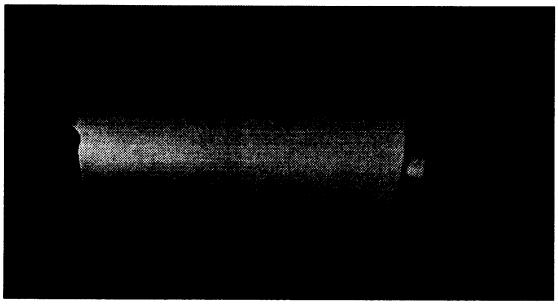

(3) B_c = 1.0 T

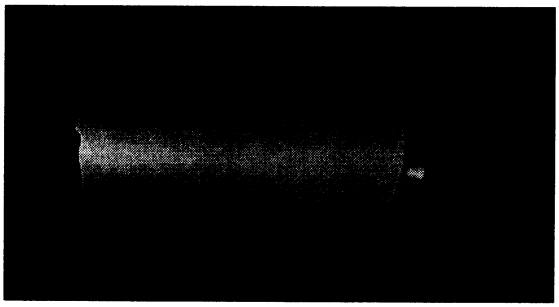

(4) B_c = 1.25 T

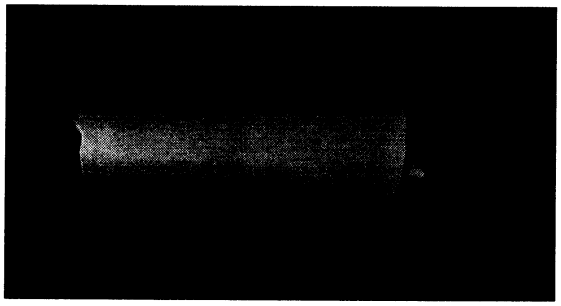

(5) B_c = 1.5 T

$\dot{m}$ =1.23±0.02 g/s, p =410±30 Pa, i_s =250 A and L = 300mm

Fig. 10 View through downstream window

On the other hand, the strong magnetic field has much less influence on the Mach disk location than the supplied current. However, the disk slightly moves in closer to the magnet as indicated in Fig. 8. This result suggests that the so-called pumping force, or pinching force, is induced by the strong magnetic field and that it acts inwardly on the jet even in the location of the Mach disk. Consequently, the disk is slightly pushed out downstream.

Figure 9 illustrates the plasma jet observed through the center window. The conditions were the same as those in Fig. 5 except for L = 300mm. It is shown in this figure that the plasma in this region contracts evidently with the application of magnetic field. The brightness in the middle of the jet around here increases with the field strength. It is also clear that the brightness in the middle of the picture for applied magnetic field intensifies compared with that for no magnetic field.

The plasma jet observed through the downstream window is illustrated in Fig. 10. It is indicated that the width of the jet, appeared in the middle and run out of the magnet bore, reduces with the application of strong magnetic field. It is similar to the pictures through the downstream window. The brightness in the middle part for applied magnetic field clearly rises compared with that for no magnetic field. Also, brighter part in the middle of the jet glows downstream. That is, the high temperature region is extended to downstream direction. These results from the aforementioned observation also show that the temperature in the plasma jet varies obviously with the intensity of magnetic field; consequently, the energy density in the plasma jet could be controlled considerably by the strong magnetic field.

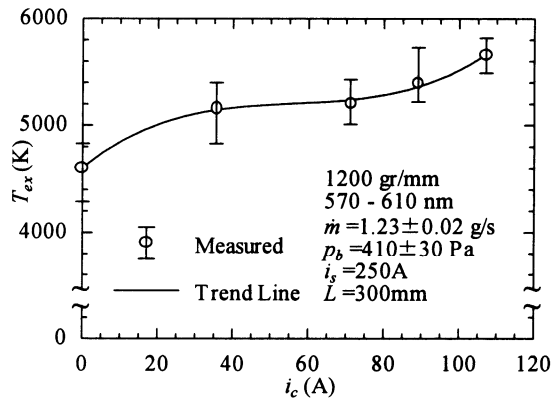

Fig. 11 Relationship between excitation temperature and specified current
(In the case of both coils' operation)

As an example of the results from the relative line intensity measurement, Fig. 11 illustrates the evolution of the excitation temperature as a function

of the specified current of superconducting coil in the case that both coils operate under the conditions of $\dot{m}$ =1.23±0.02 g/s, p =410±30 Pa, i_s =250 A and L = 300mm. The data described here were obtained by scanning the monochromator from 570 to 610 nm in wavelength. It is indicated that the excitation temperature at the measuring point increases with the specified current, that is, the strength of magnetic field. Thus, it is suggested that high temperature region in the middle of the plasma jet becomes long as the field strength increases. The pictures shot through the center window support the results obtained here. In addition, it is confirmed by these facts that the energy density in the plasma jet is controllable by the strong magnetic field.

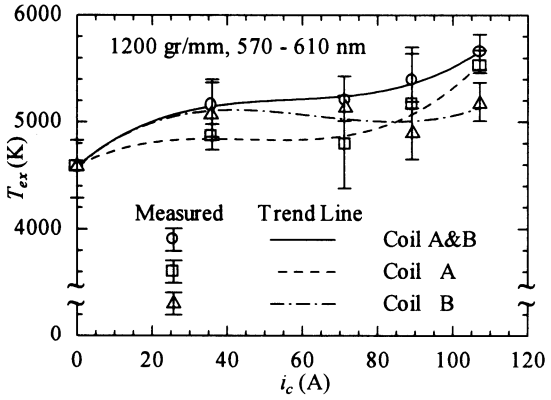

$\dot{m}$ =1.23±0.02 g/s, p =410±30 Pa, i_s =250 A and L = 300mm

Fig. 12 Relationship between excitation temperature and specified current (Influence of coil operating condition)

Moreover, the relative line intensity measurement was also conducted for a variety of coils operating conditions. In Fig. 12, a relationship between the excitation temperature and the specified current of coil is illustrated under the same conditions as Fig. 11. The results in the case of upstream coil operation, indicated in squares and broken line, show the same trend as those in the case of both coils operation, represented by circles and solid line; that is, the temperature increases with the specified current. Therefore, it is thought that the upstream coil contributes more to the flow characteristics than the downstream coil.

Conclusion

Fundamental studies are carried out as a first step to enhance the performance of plasma propulsion by the strong magnetic field. The results obtained here are summarized as follows.

(1) It is indicated from the observation using a digital video camera that the plasma jet has a typical structure of under-expanded supersonic jet. With the application of the strong magnetic field, the width of the jet reduces and, consequently, the high temperature region, located in the middle of the jet, is extended to downstream direction. Moreover, the high temperature region in the middle of the jet becomes much brighter with strong magnetic field than that without magnetic field.
(2) It is also clarified from the relative line intensity measurement that the excitation temperature at the measuring position increases with the strength of magnetic field.
(3) It is expected from these results that the energy density in the plasma jet can be controlled properly by the strong magnetic field.

Acknowledgement

This research was partly supported by a Grant-in-Aid for Scientific Research from the Ministry of Education, Science and Culture in Japan. The authors would like to thank Mr. Takashi Uno for his help in the present experiment.

References

[1] Kamiyama, S., "Application of Functional Fluids in a Magnetic Field," *Journal of the Japan Society of Mechanical Engineers*, Vol. 96, No. 899, 1993, pp. 896-899.
[2] Sato, T., Nishiyama, H. and Kamiyama, S., "Control of a Non-equilibrium Plasma Jet by Applying the Magnetic Field (Effects of Magnetic Field Distribution)," *Transactions of the Japan Society of Mechanical Engineers*, B, Vol. 60, No. 572, 1994, pp.1161-1167.
[3] Nishiyama, H., Sato, T., Veefkind, A. and Kamiyama, S., "Functional Enhancement of a Nonequilibrium Plasma Jet by Seeding in the Applied Magnetic," *Heat and Mass Transfer*, Vol. 30, No. 5, 1995, pp. 291-296.
[4] Sato, T., Nishiyama, H. and Kamiyama, S., "Effect of Magnetic Field on Turbulence of Nonequilibrium Plasma Jet in Pipe," *Transactions of the Japan Society of Mechanical Engineers,* B, Vol. 61, No. 588, 1995, pp. 2911-2917.
[5] Sato, T., Nishiyama, H. and Kamiyama, S., "Electromagnetic Control of a Nonequilibrium Plasma Jet Impinging on a Flat Plate," *Transactions of the Japan Society of Mechanical Engineers*, B, Vol. 62, No. 594, 1996, pp.519-526.